RSC Advances

ROYAL SOCIETY OF CHEMISTRY

www.rsc.org/advances

Graphical Abstract

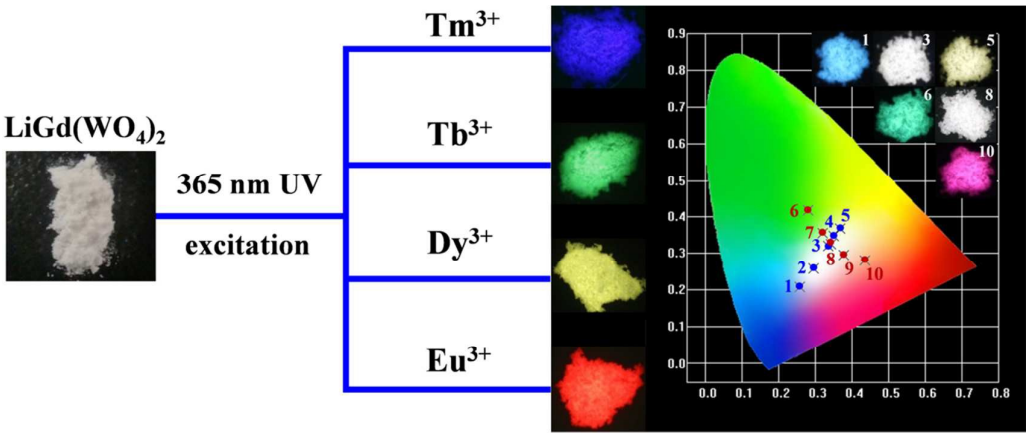

Novel single-phase white-light-emitting phosphors have been successfully synthesized by solid-state reaction and their photoluminescence properties and energy transfer mechanism have been carefully investigated.

Cite this: DOI: 10.1039/c0xx00000x

www.rsc.org/xxxxxx

ARTICLE TYPE

Tunable white-light emission *via* energy transfer in single-phase $LiGd(WO_4)_2$:Re^{3+}(Re=Tm, Tb, Dy, Eu) phosphors for UV-excited WLEDs

Yang Zhang,[a] Weitao Gong,*[a] Jingjie Yu,[b] Yuan Lin,[a] Guiling Ning*[a]

Received (in XXX, XXX) Xth XXXXXXXXX 20XX, Accepted Xth XXXXXXXXX 20XX

DOI: 10.1039/b000000x

A series of novel single-phase color tunable $LiGd(WO_4)_2$(LGW): Re^{3+} (Re=Tm, Tb, Dy, Eu) phosphors have been synthesized by solid-state reaction. The X-ray diffraction (XRD), FT-IR, photoluminescence (PL) and fluorescent decay curves were utilized to characterize the as-prepared samples. Under the excitation of UV light, LGW: Tm^{3+}, LGW: Tb^{3+}, LGW: Dy^{3+} and LGW: Eu^{3+} exhibit the characteristic emissions of Tm^{3+} (blue), Tb^{3+} (green), Dy^{3+} (yellow) and Eu^{3+} (red), respectively. On the one hand, by simply adjusting the doping concentration of Eu^{3+} ions in LGW: 2%Tm^{3+}, 4%Tb^{3+}, xEu^{3+} system, a white emission in a single-phase was achieved by blending simultaneous blue, green, and red emission of Tm^{3+}, Tb^{3+}, and Eu^{3+} ions in LGW host, in which the energy transfer from Tb^{3+} to Eu^{3+} ions was found to play an important role. On the other hand, a white emission can also be realized based on energy transfer from Tm^{3+} to Dy^{3+} ions in LGW: 2%Tm^{3+}, x%Dy^{3+} system. The energy transfer mechanism from Tm^{3+} to Dy^{3+} ions have been demonstrated to be the dipole−quadrupole interaction and the critical distance (R_{Tm-Dy}) calculated by concentration quenching method is 16.03 Å. The PL properties of as-prepared materials indicate that LGW: Re^{3+} (Re=Tm, Tb, Dy, Eu) may be potentially applied as single-phase white-light-emitting phosphors for UV-excited WLEDs.

1. Introduction

Nowadays, with the continuously increasing of global electricity consumption in artificial lighting, the development of new high-efficiency lighting sources has become particularly important for reducing the world's energy consumption.[1-4] As a hot spot in the field of solid-state lighting applications, white light-emitting diodes (WLEDs) have expected as the most promising long-term solution due to their attractive merits of energy savings, longer lifetimes (>100000h), faster response, higher luminous efficiency and environmental friendliness compared with conventional incandescent and fluorescence lamps.[5-7] The 2014 Nobel Prize in Physics has been awarded to Isamu Akasaki, Hiroshi Amano and Shuji Nakamura "for the invention of efficient blue light-emitting diodes which has enabled bright and energy-saving white light sources" adequately affirmed this technology.[8] Currently, the most common method for producing commercial WLEDs are based on a blue-emitting InGaN LED chip with a yellow-emitting phosphor (YAG: Ce^{3+}). Despite their wide applications and high luminous efficacy (>100 lm W^{-1}), the major disadvantage of such a combination is that they are limited to high correlated color temperature (CCT > 6000K) and low color rendering index (R_a < 80) due to the lack of sufficient red spectral component, which restricts their widespread commercialization in general lighting market.[9-11] This limitation can be solved by utilizing an ultraviolet (UV) light-emitting diode (LED) chip coated with multiphased phosphors emitting blue, green, and red light. However, the fatal shortcoming of this method is the relatively low luminescent efficiency owing to the strong reabsorption of the blue light by the red and green phosphors.[12-14] Moreover, the multiphosphors systems are difficult to make, because the phosphors have to be prepared separately, the particle sizes of individual phosphor materials have to be adapted to one another in order to avoid agglomeration or sedimentation, and the final product has to be mixed very homogeneously in exact ratios.[8] To solve the above challenges, recently, single-phase white-light-emitting phosphors pumped by UV or near-UV LED chips have attracted great interest and been considered as an effective approach for phosphor-converted WLEDs, since they show significant advantages compared with the multiphased phosphors, including higher luminescence efficiency, higher color rendering index, better reproducibility, lower manufacturing costs and a more easily fabrication process.[15-18]

The most widely used method to realize white light in a single-phased phosphor is by codoping sensitizer and activator into the same host matrix. It should be pointed out that energy transfer plays a critical role in achieving white light emission in a single-phase phosphor. As a result, single-phase white-light-emitting phosphors based on the mechanism of energy transfer from a sensitizer to an activator have been realized in many inorganic hosts, such as $NaCaBO_3$: Ce^{3+}, Tb^{3+}, Mn^{2+},[19] $Na_2Ca_4Mg_2Si_4O_{15}$: Eu^{2+}, Mn^{2+},[20] $Ca_4(PO_4)_2O$: Ce^{3+}, Eu^{2+},[21] $BaY_2Si_3O_{10}$: Ce^{3+}, Tb^{3+}, Eu^{3+},[22] $Sr_7La_3[(PO_4)_{2.5}(SiO_4)_3(BO_4)_{0.5}](BO_2)$: Ce^{3+}, Mn^{2+},[23] and so on. However, some harsh reaction conditions such as high temperature (above 1000 °C) and reducing atmosphere

especially for Eu^{2+} or Ce^{3+} ions doped phosphors leading to a high investment and energy costs. So, it will be interesting to find a new single-phase white-light phosphor which can be synthesized at a moderate temperature and in an ambient atmosphere. Recently, scheelite-like double tungstate with the general formula of $MRe(WO_4)_2$ (M = alkali metal, Re = rare earth) phosphors for WLEDs applications have gained increasing interest for their promising luminescent properties, excellent physical and chemical stability, low synthetic temperature, and environmentally friendly characteristics.[24-27] In addition, the optical properties of these materials can be well improved due to their strong ultraviolet absorption capacity and effectively transfer the absorbed energy to the doping ions.

In this research, a series of novel single-phase $LiGd(WO_4)_2$(LGW) phosphors with tunable emission color through singly doping or codoping rare earth ions (Tm^{3+}, Tb^{3+}, Dy^{3+}, and Eu^{3+}) have been successfully synthesized by solid-state reaction. We find that LGW: Tm^{3+} phosphors show blue emission under the excitation of 360 nm, which match well with the emission light of UV-LED chips. Furthermore, two routes are discovered to realize the white emission in single LGW host. When codoping Tm^{3+}, Tb^{3+}, and Eu^{3+} ions into LGW host, a white emission is realized by simply adjusting the doping concentration of Eu^{3+} ions, in which the energy transfer from Tb^{3+} to Eu^{3+} ions was found to play an important role. On the other hand, a white emission can also be achieved by utilizing the principle of energy transfer and appropriate tuning of Tm^{3+} and Dy^{3+} contents in LGW: Tm^{3+}, Dy^{3+}. Moreover, we investigate the energy transfer mechanism between Tm^{3+} and Dy^{3+} ions in LGW: Tm^{3+}, Dy^{3+}, which results in the tunable emission colors from such phosphor materials. These results indicate that the as-prepared products may be potentially applied as candidates of single-phase white-light-emitting phosphors for application in WLEDs.

2. Experimental

2.1 Materials and Synthesis

A series of rare-earth-doped $LiGd(WO_4)_2$ phosphors were synthesized through the solid-state reaction. The Li_2CO_3 (A.R.), WO_3 (A.R.), Gd_2O_3 (99.99%), Tm_2O_3 (99.99%), Tb_4O_7 (99.99%), Dy_2O_3 (99.99%) and Eu_2O_3 (99.99%) were used as the starting materials. The stoichiometric amounts of the raw materials were first thoroughly mixed by grinding them in an agate mortar with an appropriate amount of ethanol and then dried at 80 °C for 0.5 h. After reground for 10 min, the powder mixtures were loaded into the crucible and transferred to the box furnace to calcine at 800 °C for 6 h in air condition with a heating rate of 3 °C min^{-1}. Finally, the prepared samples were cooled to room temperature and then ground once more for further measurements.

2.2 Characterization

The X-ray diffraction (XRD) patterns of the samples were recorded on a Rigaku D/max 2400 X-ray diffractometer using Cu Kα radiation(λ= 0.15405 nm). Fourier transform infrared (FTIR) spectra were performed on a JASCO FT/IR-460 plus spectrometer using a KBr disk technique. Photoluminescence (PL) emission and photoluminescence excitation (PLE) spectra as well as quantum efficiency were carried out on a Hitachi F-7000 spectrophotometer equipped with a 150 W xenon lamp as the excitation source. The luminescent decay curves were measured using an FLS920 spectrofluorometer (Edinburgh Instruments). All the measurements were performed at room temperature.

3. Result and discussion

3.1 Phase Identification and Structure

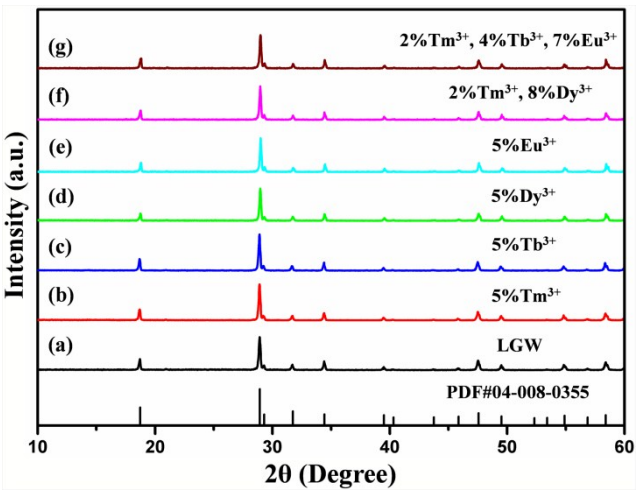

Fig. 1 XRD patterns of representative LGW host (a), LGW: 5%Tm^{3+} (b), LGW: 5%Tb^{3+} (c), LGW: 5%Dy^{3+} (d), LGW: 5%Eu^{3+} (e), LGW: 2%Tm^{3+}, 8%Dy^{3+} (f), LGW: 2%Tm^{3+}, 4%Tb^{3+}, 7%Eu^{3+} (g) samples and the standard data of $LiGd(WO_4)_2$ (JCPDS no. 04-008-0355).

The representative XRD patterns of LGW and Tm^{3+}, Tb^{3+}, Dy^{3+}, Eu^{3+} ions doped LGW samples as well as the standard data of $LiGd(WO_4)_2$ (JCPDS no. 04-008-0355) are presented in Fig. 1. It is obvious that the diffraction peaks of all these samples are well assigned to the pure tetragonal phase of $LiGd(WO_4)_2$ [space group: $I4_1/a$ (88)] according to JCPDS file 04-008-0355, and no traces of impurity phases are observed, indicating that the Tm^{3+}, Tb^{3+}, Dy^{3+} and Eu^{3+} ions can be completely dissolved into this host and their introductions do not cause any significant changes to the crystal structure. The $LiGd(WO_4)_2$ crystallizes belongs to a

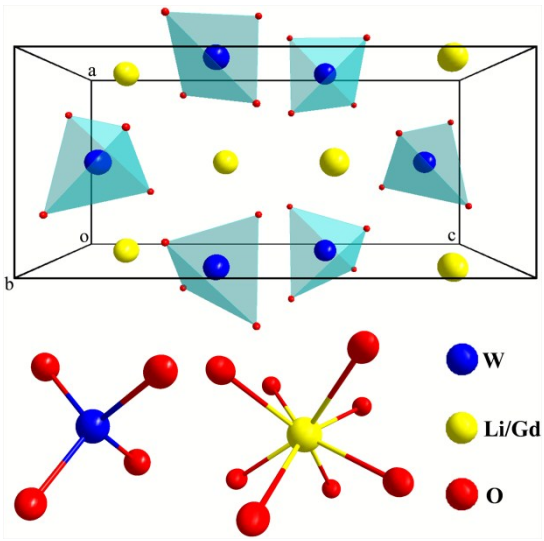

Fig. 2 The unit cell structure of LGW and the coordination environment of cations in the host lattice.

scheelite-type tetragonal structure, which has the cell parameters of $a = b = 5.20$ Å, $c = 11.17$ Å, $V = 302.03$ Å^3 and $Z = 2$.[28] Fig. 2 shows the unit cell structure of $LiGd(WO_4)_2$ and the coordination environments of the Gd^{3+} (Li^+) and W^{2+} sites. It can be seen that the central W^{6+} is coordinated by four oxygen atoms at a tetrahedral site, the Li^+ and Gd^{3+} cations are randomly distributed over the same site positions and are coordinated by eight oxygen atoms to form a distorted polyhedron with symmetry S_4 (without an inversion center).[29-31] Based on the similar effective ionic radii and charge balance, the Tm^{3+}, Tb^{3+}, Dy^{3+} and Eu^{3+} ions are expected to occupy Gd^{3+} sites in the $LiGd(WO_4)_2$.

To determine the chemical constituents of sample, FT-IR spectroscopy is performed on the pure LGW phosphor, as shown in Fig. 3. A broad absorption band at 3395 cm^{-1} is ascribed to the stretching vibration of O–H, which belongs to physical absorbed water on the surface of product from air. And a weak absorption band at 1652 cm^{-1} is attributed to the bending vibration of O–H. The set of bands below 1000 cm^{-1} are characteristic vibrations of W–O bands (from the WO_4^{2-} group). A strong absorption band at 808 cm^{-1} and a weak band at 443 cm^{-1} are caused by the stretching vibration of W–O and bending vibration of W–O, respectively.[32]

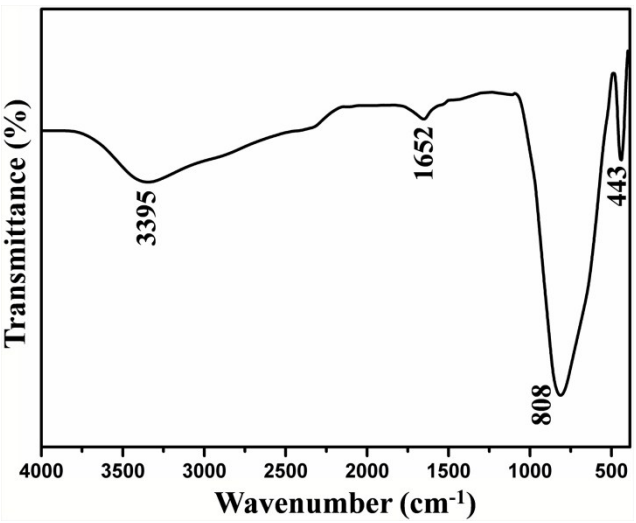

Fig. 3 FT-IR spectra of the pure LGW

3.2 Photoluminescence Properties

Fig. 4 illustrates the PLE and PL spectra of LGW: 5%Tm^{3+}, LGW: 5%Tb^{3+}, LGW: 5%Dy^{3+} and LGW: 5%Eu^{3+} samples, respectively. The excitation spectrum of LGW:5%Tm^{3+} exhibited in Fig. 4a contains a sharp absorption peak at 360 nm attributed to the $^3H_6 \rightarrow {}^1D_2$ transition of Tm^{3+},[33] which matches well with the UV-LED chips. Upon excitation at 360 nm, the LGW: 5%Tm^{3+} phosphor shows an intense blue emission attributed to the $^1D_2 \rightarrow {}^3F_4$ transition (455 nm),[34] indicating it could be an outstanding candidate in blue phosphor for UV-LED chips. Fig. 4b shows the PL excitation and emission spectra of LGW: 5%Tb^{3+} phosphors. The excitation spectrum was obtained by monitoring the emission of Tb^{3+} (547 nm, $^5D_4 \rightarrow {}^7F_5$). It is observed that the excitation spectrum can be divided into two parts: one is a broad band with a maximum at 272 nm, which is attributed to the charge-transfer absorption from the 2p orbitals of the oxygens to the 5d orbitals of tungsten within the WO_4^{2-} groups and the $4f^8 \rightarrow 4f^7 5d$ transition of Tb^{3+};[35] the other one is composed of a series of narrow bands from 300 to 400 nm, which correspond to the characteristic f−f transitions of Tb^{3+} within its $4f^8$ configuration.[25] Under 272 nm excitation, the obtained emission spectrum of LGW: 5%Tb^{3+} consists of f–f transition lines within $4f^8$ electron configuration of Tb^{3+}, *i.e.*, $^5D_4 \rightarrow {}^7F_6$ (490 nm) in the blue region and $^5D_4 \rightarrow {}^7F_5$ (547 nm) in the green region, as well as $^5D_4 \rightarrow {}^7F_4$ (590 nm), $^5D_4 \rightarrow {}^7F_3$ (623 nm) in the red region.[36] The strongest one is located at 547 nm corresponding to $^5D_4 \rightarrow {}^7F_5$ transition of Tb^{3+}. As for LGW:5%Dy^{3+} phosphors, the excitation spectra monitoring the emission at 576 nm corresponding to $^4F_{9/2} \rightarrow {}^6H_{13/2}$ transition of Dy^{3+} is shown in Fig. 4c. It can be seen that the excitation spectrum of the LGW:5%Dy^{3+} consists of a strong broad band from 200 to 320 nm with a maximum at 267 nm due to the WO_4^{2-} groups as discussed above. In the longer wavelength region from 310 to 500 nm, some sharp lines due to the f–f transitions of Dy^{3+}

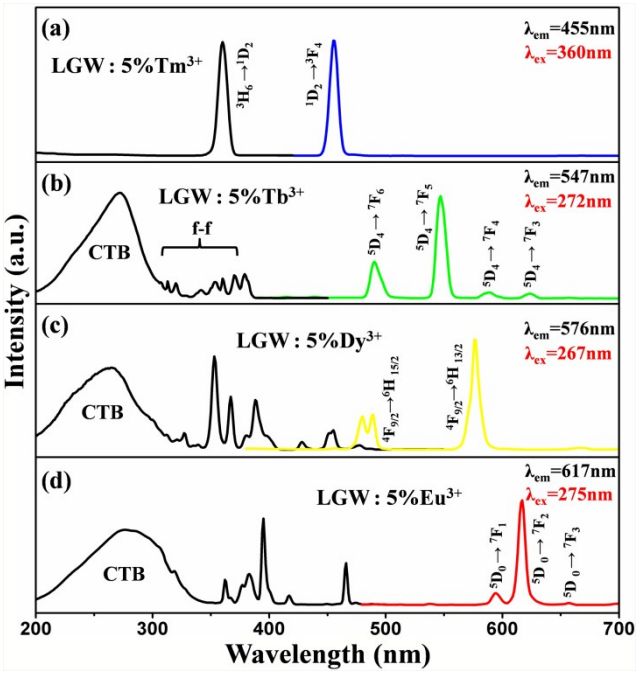

Fig. 4 PL and PLE spectra of (a) LGW: 5%Tm^{3+}, (b) LGW: 5%Tb^{3+}, (c) LGW: 5%Dy^{3+} and (d) LGW: 5%Eu^{3+} samples.

are observed, which are ascribed to the transitions from the $^6H_{15/2}$ ground state to the different excited states of Dy^{3+}, *i.e.*, 327 nm ($^6P_{3/2}$), 353 nm ($^6P_{7/2}$), 367 nm ($^6P_{5/2}$), 388 nm ($^4I_{13/2}$), 428 nm ($^4G_{11/2}$), 455 nm ($^4I_{15/2}$), 477 nm ($^4F_{9/2}$), respectively.[37] Upon the excitation at 267 nm, LGW:5%Dy^{3+} phosphors obtain blue and yellow luminescence, corresponding to the $^4F_{9/2} \rightarrow {}^6H_{15/2}$ (478 and 488 nm) and the $^4F_{9/2} \rightarrow {}^6H_{13/2}$ (576 nm) transitions of Dy^{3+} ions, respectively. The $^4F_{9/2} \rightarrow {}^6H_{15/2}$ transition is the magnetic dipole transition, which hardly varies with the crystal field strength or coordination environment around the Dy^{3+} ions. However, the forced electric dipole transition $^4F_{9/2} \rightarrow {}^6H_{13/2}$ transition ($\Delta J = 2$) is hypersensitive to the chemical environment around the Dy^{3+} ions in the host lattice.[38] When the Dy^{3+} ions locate at low-symmetry sites without inversion center, the yellow emission $^4F_{9/2} \rightarrow {}^6H_{13/2}$ transition is often prominent in the emission spectra. From the results in Fig. 4c (right), the intensity

of the $^4F_{9/2} \rightarrow {}^6H_{13/2}$ transition is much stronger than that of the $^4F_{9/2} \rightarrow {}^6H_{15/2}$ transition, indicating that Dy^{3+} ions are located in an asymmetric cation environment, which is consistent with a symmetry S_4 without an inversion center. At last, Fig. 4d shows the PL excitation and emission spectra of LGW: 5%Eu^{3+} phosphors. When monitoring by the red emission of Eu^{3+} (617 nm, $^5D_0 \rightarrow {}^7F_2$), the PLE spectrum of LGW: 5%Eu^{3+} reveals a broad band ranging from 200 to 350 nm ascribed to the CTB of the WO_4^{2-} groups and $O^{2-} - Eu^{3+}$ charge transfer transition from an oxygen 2p state excited to an Eu^{3+} 4f state.[26] In addition, we can easily distinguish the characteristic lines located at 362, 383, 395, 417, 466 nm corresponding to the transitions of Eu^{3+} ion from the ground level $^7F_0$ to the $^5D_4$, $^5L_7$, $^5L_6$, $^5D_3$, and $^5D_2$ excited levels, respectively.[39] The PL spectrum of LGW: 5%Eu^{3+} phosphor is obtained by exciting at 275 nm. It can be found that the strongest emission peak of LGW: 5%Eu^{3+} is located at 617 nm, which originates from the $^5D_0 \rightarrow {}^7F_2$ transition of Eu^{3+}. Other two weak peaks at 594 and 657 nm are attributed to the $^5D_0 \rightarrow {}^7F_1$ and $^5D_0 \rightarrow {}^7F_3$ transitions of Eu^{3+}, respectively. It is well-known that Eu^{3+} is an excellent structural probe for investigating the local environment in a host lattice. The electric dipole transition $^5D_0 \rightarrow {}^7F_2$ is a hypersensitive one, and the emission intensity is strongly influenced by local environment surrounding Eu^{3+} ions. When Eu^{3+} ions are located at a low symmetry site, the $^5D_0 \rightarrow {}^7F_2$ transition often dominates in the emission spectrum. Nevertheless, the magnetic dipole transition ($^5D_0 \rightarrow {}^7F_1$) is independent from the local crystal field environment.[40] In the present case, the emission intensity of electric transition is much stronger than that of magnetic dipole transition, indicating that the Eu^{3+} ions occupy the low symmetry sites, which is in accord with the emission spectrum of the LGW: 5%Dy^{3+}. As illustrated in Fig. 4a,b,c,d, there are some excitation peaks from 350 to 420 nm in the PLE spectrum of Tm^{3+}, Tb^{3+}, Dy^{3+} and Eu^{3+} doped LGW samples, which indicates that those phosphors can match well with the dominant emission band of a UV-LED chip. In addition, the presence of the excitation peak of the WO_4^{2-} groups in the excitation spectrum of $Tb^{3+}/Dy^{3+}/Eu^{3+}$ implies that there is an energy transfer from WO_4^{2-} groups of host to $Tb^{3+}/Dy^{3+}/Eu^{3+}$ ions in phosphors.[41] However, we does not observe a charge transfer band for WO_4^{2-} groups in the PLE spectrum of LGW:Tm^{3+}, certifying the inexistence of the energy transfer from WO_4^{2-} to Tm^{3+}.

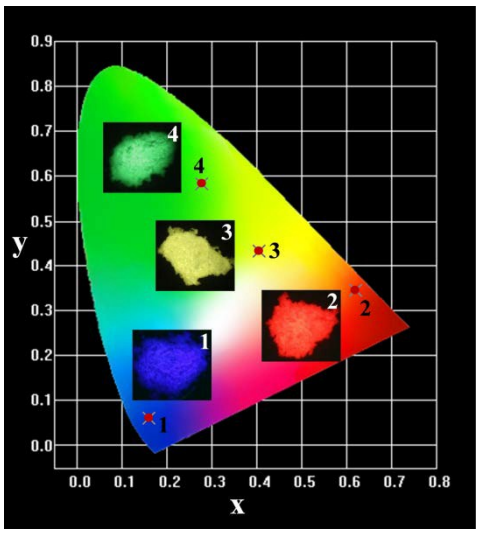

Fig. 5 CIE color coordinate diagram of LGW doped with 5% (1) Tm^{3+}, (2) Eu^{3+}, (3) Dy^{3+}, and (4) Tb^{3+}. The insets are their corresponding digital photographs taken under 365 nm excitation.

A better understanding of the actual emission color of the phosphor is very important in the applications of lighting and display devices. Fig. 5 shows the Commission International de L'Eclairage (CIE) chromaticity coordinates and the corresponding digital luminescence photographs of LGW: 5%Tm^{3+}, LGW: 5%Tb^{3+}, LGW: 5%Dy^{3+} and LGW: 5%Eu^{3+} phosphors. The CIE chromaticity coordinates of LGW: $Tm^{3+}/Tb^{3+}/Dy^{3+}/Eu^{3+}$ phosphors can vary from (0.160, 0.061) for LGW: 5%Tm^{3+} to (0.277, 0.583) for LGW:5%Tb^{3+}, (0.406, 0.431) for LGW: 5%Dy^{3+}, and (0.619, 0.345) for LGW:5%Eu^{3+}, which correspond to the color changes from blue to green, yellow, and red, respectively.

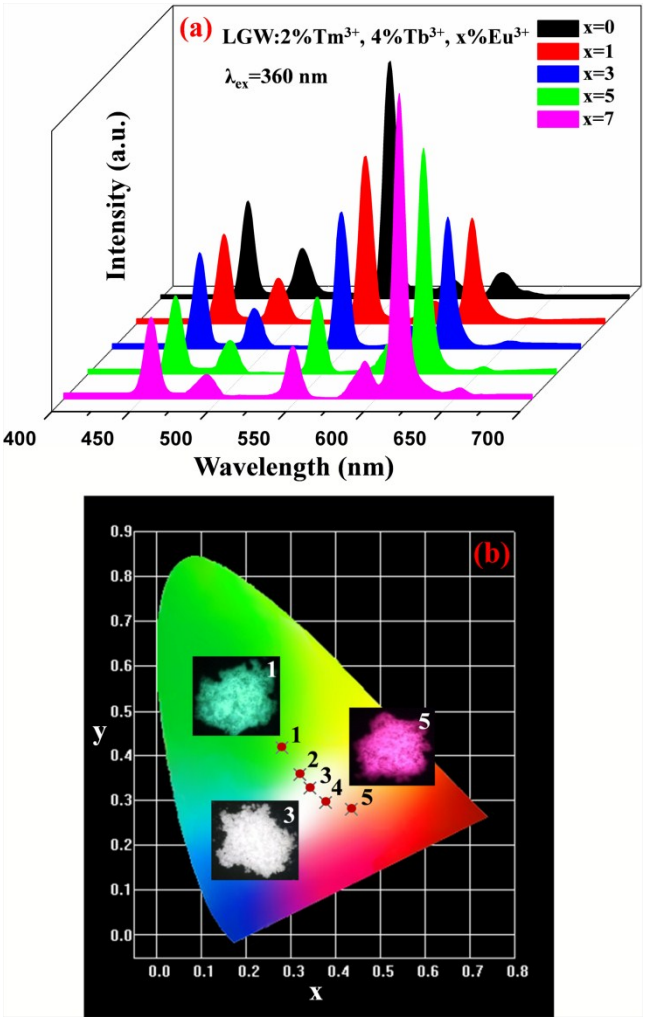

Fig. 6 (a) PL emission spectra of LGW: 2%Tm^{3+}, 4%Tb^{3+}, x%Eu^{3+} samples with different Eu^{3+} concentrations ($0 \leq x \leq 7$). (b) CIE coordinate diagram of LGW: 2%Tm^{3+}, 4Tb^{3+}, x%Eu^{3+} with different Eu^{3+} concentrations: (1) x = 0; (2) x = 1; (3) x = 3; (4) x = 5; and (5) x = 7. The insets are their corresponding digital photographs taken under 365 nm excitation.

The aim of this study is to realize the white light emission in a single-phase host for UV-excited WLEDs. For this purpose, an

appropriate amounts combination of the luminescent ions Tm^{3+}, Tb^{3+}, and Eu^{3+} as emitters of blue, green, and red light codoped into LGW host was selected for white light generation. Therefore, a series of LGW: 2%Tm^{3+}, 4%Tb^{3+}, x%Eu^{3+} (x = 0, 1, 3, 5, 7) samples have been prepared. The PL spectra of the as-prepared samples under excitation at 360 nm and the corresponding CIE chromaticity diagram are presented in Fig. 6. Under the excitation of 360 nm, the emission color varies from light green (which is represented at point 1) to rose red (point 5), and especially the white light is realized (points 3) by simply controlling the doping concentration of Eu^{3+} ions (Fig. 6b). Therefore, a novel single-phase white-emitting phosphor is successfully obtained by blending simultaneous blue, green, and red emission of Tm^{3+}, Tb^{3+}, and Eu^{3+} ions in LGW host under UV light excitation.

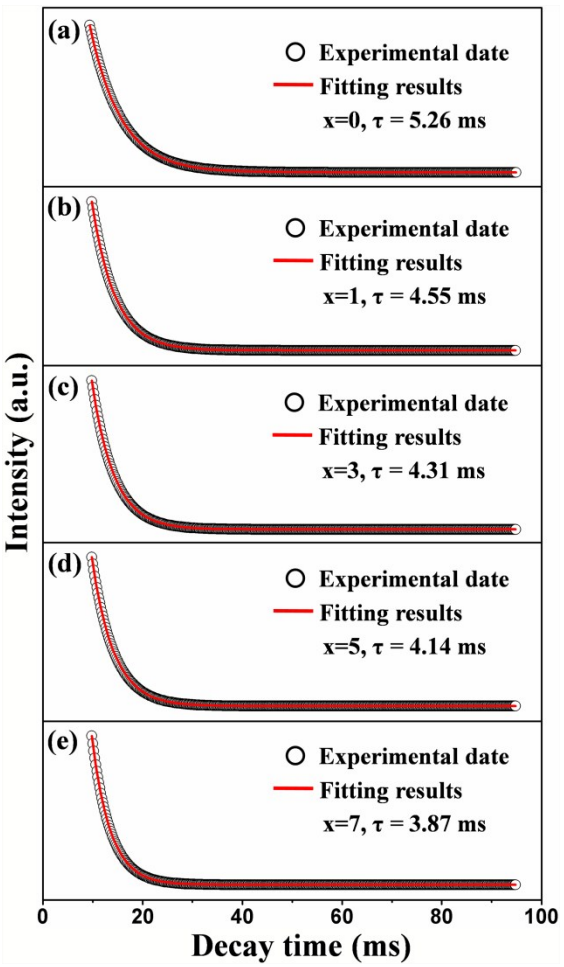

Fig. 7 The decay curves for the luminescence of Tb^{3+} ions in LGW: 2%Tm^{3+}, 4%Tb^{3+}, x%Eu^{3+} with changing Eu^{3+} concentrations (excited at 272 nm, monitored at 547 nm).

Detailed information of LGW: 2%Tm^{3+}, 4%Tb^{3+}, x%Eu^{3+} (x = 0, 1, 3, 5, 7) phosphors for the CIE chromaticity coordinates and CCTs are listed in Table 1. Moreover, it is worthy to note that although the concentration of Tb^{3+} was fixed at 4%, as the Eu^{3+}-doping concentration increased, the emission intensity of Eu^{3+} was enhanced clearly whereas the emission intensity of Tb^{3+} decreased monotonously (Fig. 6a), indicating that there is an energy transfer process from the Tb^{3+} to Eu^{3+} ions. As reported, the luminescence intensities of various rare earth ions can be

Table 1 Comparison of the CIE chromaticity coordinates and CCT (K) for LGW:2%Tm^{3+}, 4%Tb^{3+}, x%Eu^{3+} phosphors excited under 360 nm UV radiation

Sample no	Sample composition	CIE coordinates (x, y)	CCT(K)
1	x=0	(0.279,0.418)	7344
2	x=1	(0.321,0.356)	5993
3	x=3	(0.343,0.327)	4980
4	x=5	(0.377,0.296)	3159
5	x=7	(0.435,0.280)	1961

enhanced or quenched by energy transfer from other codoping rare earth ions.[42] Energy transfer between Tb^{3+} and Eu^{3+} is a well-known phenomenon since the $^5D_4 \rightarrow {}^7F_{6,\,5,\,4,\,3}$ emissions of Tb^{3+} are effectively overlapped with the $^7F_{0,\,1} \rightarrow {}^5D_{0,\,1,\,2}$ absorptions of Eu^{3+}.[43] So far, the energy transfer phenomenon from Tb^{3+} to Eu^{3+} has been extensively investigated in many inorganic hosts, such as molybdates,[36] fluorides,[44] germanates,[45] tungstates,[46] oxyhalides,[47] niobates,[48] and so on. In order to provide further evidence to validate the energy transfer from Tb^{3+} to Eu^{3+} ions in the LGW host lattice, the fluorescence decay curves of Tb^{3+} in the LGW: 2%Tm^{3+}, 4%Tb^{3+}, x%Eu^{3+} ($0 \le x \le 7$) samples excited at 272 nm, monitoring the emission of the Tb^{3+} ions at 547 nm, were measured and shown in Fig. 7. The decay curves fit well with a single exponential formula as follows:[49]

$$I = I_0 \exp(-t/\tau) \quad (1)$$

where I and I_0 are the luminescence intensities at time t and 0, and τ is the luminescence lifetime. For the LGW: 2%Tm^{3+}, 4%Tb^{3+}, x%Eu^{3+} ($0 \le x \le 7$) samples, the lifetime of Tb^{3+} decreases with increasing Eu^{3+} concentration, which are 5.26, 4.55, 4.31, 4.14 and 3.87 ms for x = 0, 1, 3, 5 and 7, respectively. This is a powerful proof for the energy transfer from Tb^{3+} to Eu^{3+} ions.

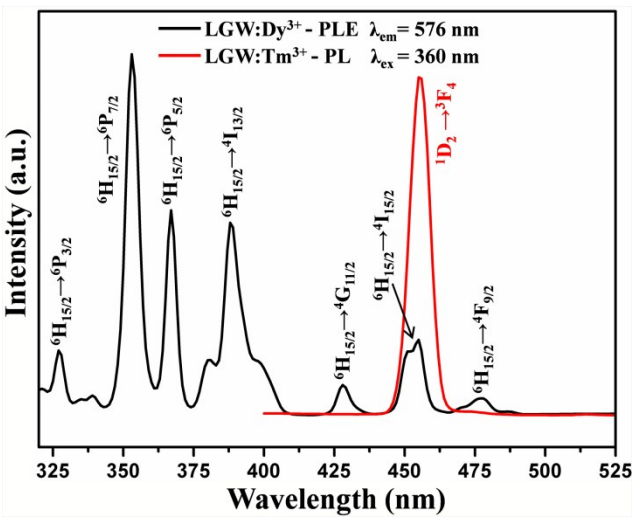

Fig. 8 Spectral overlap between the PL spectrum of LGW: Tm^{3+} (red line) and PLE spectrum of LGW: Dy^{3+} (black line).

Interestingly, white light emission can also be realized by combining the blue and yellow emissions of the Tm^{3+} and Dy^{3+} ions in a single host under UV light excitation. As shown in Fig. 8, the comparison of the PL spectrum of LGW: Tm^{3+} and PLE spectrum of LGW: Dy^{3+} reveals a significant spectral overlap between the emission of Tm^{3+} and the excitation of Dy^{3+}. Therefore, effective resonance-type energy transfer from Tm^{3+} to

Dy^{3+} in LGW host is expected. In order to further investigated the energy transfer process from Tm^{3+} to Dy^{3+} and study the impact of doping concentration on the luminescence properties of phosphors, a series of LGW: 2%Tm^{3+}, x%Dy^{3+}(x=0, 2, 4, 6, 8, 10) samples were prepared. The PL spectra of LGW: 2%Tm^{3+}, x%Dy^{3+} under 360 nm excitation are illustrated in Fig. 9. The doping concentration Tm^{3+} was fixed at 2%, while the Dy^{3+} content changes from 0% to 10%. We can observe that as the amount of Dy^{3+} doping content increases, the emission intensity of Tm^{3+} gradually decreases, whereas the emission intensity of Dy^{3+} first increases to an optimum concentration at 6%, and then begins to decrease because of the concentration quenching effect, which certifies the existence of energy transfer from Tm^{3+} to Dy^{3+} ions. Meanwhile, those single-phase LGW: 2%Tm^{3+}, x%Dy^{3+} phosphors exhibit abundant color-tunable emissions by effective energy transfer process and controlling the doping concentrations

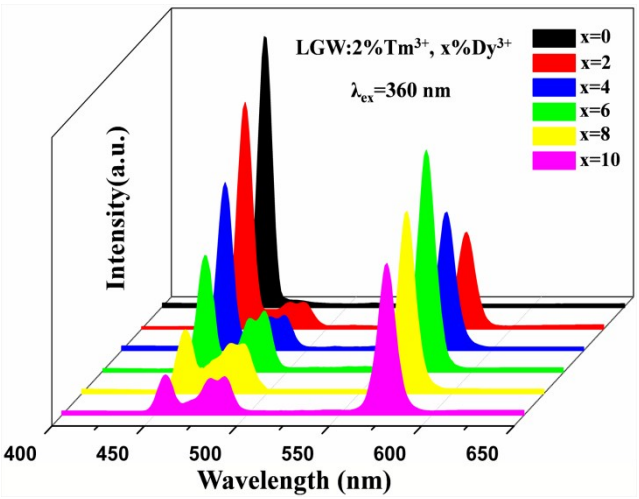

Fig. 9 PL emission spectra of LGW: 2%Tm^{3+}, x%Dy^{3+} samples with different Dy^{3+} concentrations (x = 0, 2, 4, 6, 8, 10).

of Dy^{3+}. The most interesting part of this approach is its ability to realize white light emission from a particular sample of LGW: 2%Tm^{3+}, 6%Dy^{3+}. This has been confirmed by direct exposure to ultraviolet (UV) light as well as from the CIE coordinate calculation (discussed later). In addition, the fluorescent decay lifetimes measurements for the Tm^{3+} emission (λ_{ex} = 360 nm, λ_{em} = 455 nm) with the increasing Dy^{3+} concentration in LGW: 2%Tm^{3+}, x%Dy^{3+} were conducted to further confirm the occurrence of energy transfer from Tm^{3+} to Dy^{3+}. Fig. 10 shows the decay curves of Tm^{3+} emission in the LGW: 2%Tm^{3+}, x%Dy^{3+} samples. The decay curves can be fitted successfully by a second-order exponential function as the following equation:[50]

$$I = A_1\exp(-t/\tau_1) + A_2\exp(-t/\tau_2) \quad (2)$$

where I represents the luminescent intensity; A_1 and A_2 are constants; t is the time; τ_1 and τ_2 are rapid and slow decay time for exponential components, respectively. As a result, the average decay times (τ*) can be determined using the following equation:

$$\tau^* = (A_1\tau_1^2 + A_2\tau_2^2)/(A_1\tau_1 + A_2\tau_2) \quad (3)$$

On the basis of equation 3, the average lifetimes of Tm^{3+} are determined to be 9.56, 7.82, 6.63, 5.31 and 4.54 μs for Dy^{3+} concentrations of 0%, 4%, 6%, 8%, and 10%, respectively. The decrease in the lifetimes of Tm^{3+} with increasing Dy^{3+} concentration strongly demonstrates the existence of energy transfer from Tm^{3+} to Dy^{3+} ions. Fig. 11 illustrates the schematic

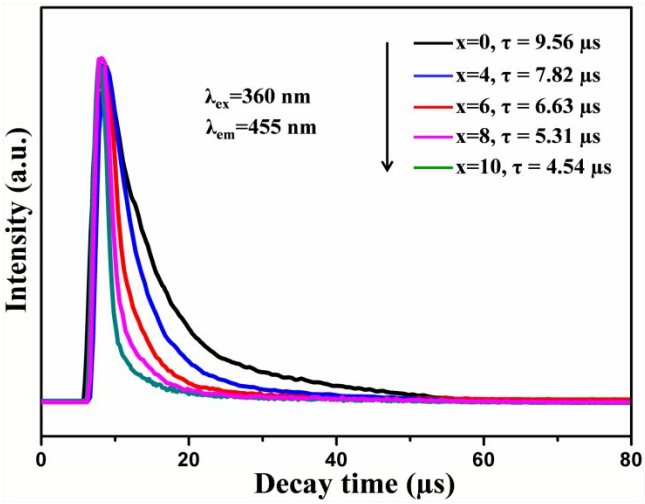

Fig. 10 Photoluminescence decay curves of Tm^{3+} in LGW: 2%Tm^{3+}, x%Dy^{3+} with changing Dy^{3+} concentrations

diagram of the energy transfer process from Tm^{3+} to Dy^{3+} in LGW: Tm^{3+}, Dy^{3+} phosphor. As shown in Fig. 11, the energy gap between $^1D_2$ and $^3F_4$ of Tm^{3+} matches well with that between $^6H_{15/2}$ and $^4I_{15/2}$ of Dy^{3+}, which makes the energy transfer from Tm^{3+} to Dy^{3+} ions efficient. Those illustrate the existence of energy transfer from Tm^{3+} to Dy^{3+} when they are codoped into the LGW host and provide a necessary condition for synthesizing the single-phase color-tunable phosphors.

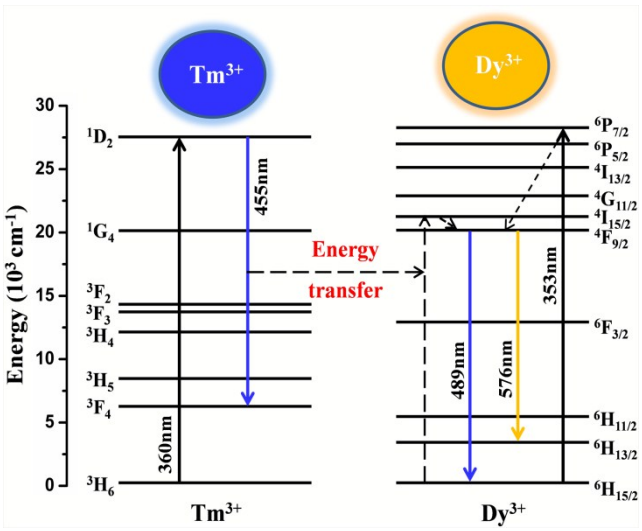

Fig. 11 A simple model expressing the energy transfer from Tm^{3+} to Dy^{3+} in LGW: Tm^{3+}, Dy^{3}.

3.3 Energy Transfer Mechanism.

The energy transfer efficiency (η_T) from Tm^{3+} to Dy^{3+} in LGW: 2%Tm^{3+}, x%Dy^{3+} systems can be calculated using the following equation:[51]

$$\eta_T = 1 - I_S/I_{S0} \quad (4)$$

where η_T is the energy transfer efficiency, and I_S and I_{S0} are the

luminescence intensities of the Tm^{3+} ions in the presence and absence of the Dy^{3+}, respectively. As shown in Fig. 12, the intensity of Tm^{3+} emission and energy transfer efficiency from Tm^{3+} to Dy^{3+} in LGW: 2%Tm^{3+}, x%Dy^{3+} system are plotted as a function of the Dy^{3+} concentration. One can find that as the increase of Dy^{3+} concentration, the intensity of Tm^{3+} emission decreases gradually, while the energy transfer efficiency monotonously increases to reach maximum at 84% when using UV irradiation of 360 nm as the excitation wavelength, indicating that the energy transfer from Tm^{3+} to the Dy^{3+} becomes more and more efficient.

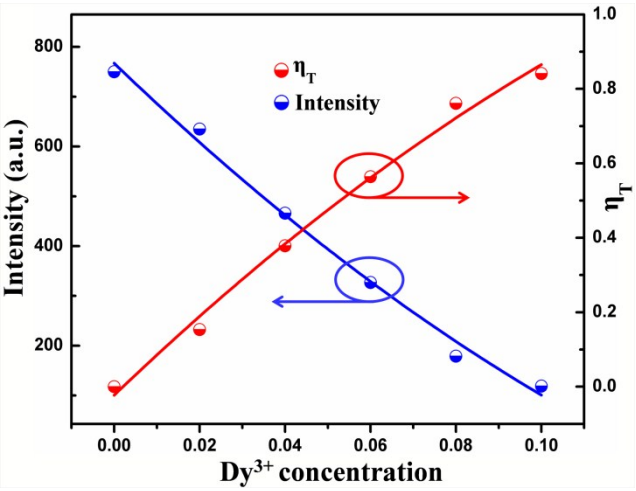

Fig. 12 Dependence of the emission intensity of Tm^{3+} and the energy transfer efficiency (η_T) on Dy^{3+} concentration in LGW:2%Tm^{3+}, x%Dy^{3+}(x = 0, 2, 4, 6, 8, 10) phosphors.

In order to determine the energy transfer mechanism from the Tm^{3+} to the Dy^{3+} ions, it is necessary to know the critical distance (R_c) between sensitizer (Tm^{3+}) and activator (Dy^{3+}). With the increase of Dy^{3+} content, the distance between Tm^{3+} and Dy^{3+} ions becomes shorter and shorter, thus the probability of energy migration increases. When the distance becomes small enough, the concentration quenching occurs and the energy migration is hindered. Therefore, the critical distance (R_c) for energy transfer from the Tm^{3+} to Dy^{3+} ions can be calculated using the concentration quenching method. According to Blasse,[52, 53] the critical distance between Tm^{3+} and Dy^{3+} ions can be expressed by

$$R_c = 2\left(\frac{3V}{4\pi X_c N}\right)^{1/3} \quad (5)$$

where V refers to the volume of the unit cell, N is the number of available sites for the dopant in the unit cell, and X_c is the total content of Tm^{3+} and Dy^{3+}, at which the luminescenc intensity of Tm^{3+} is half that of the sample in the absence of Dy^{3+} ions. For the LGW host, V = 302.03 Å^3, N = 2, and X_c =0.07. Therefore, the R_c value is calculated to be about 16.03 Å. Generally, non-radiative energy transfer from a sensitizer to an activator usually takes place through exchange interaction or electric multipolar interactions.[54] The value of R_c calculated above implies the little possibility of exchange interaction because the exchange interaction is predominant only for about 5 Å.[55] As a consequence, we can conclude the energy transfer mechanisms

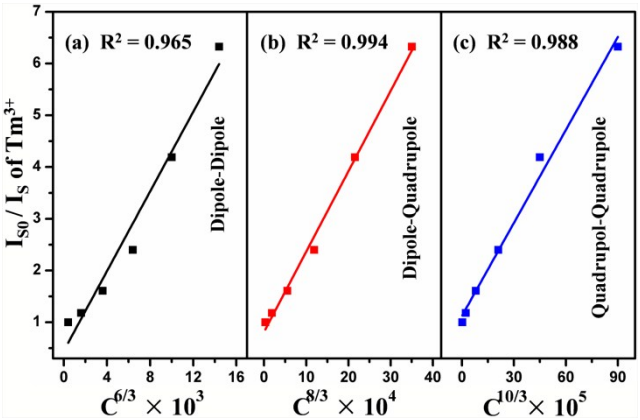

Fig. 13 Dependence of I_{S0}/I_S of Tm^{3+} emission on Tm^{3+} and Dy^{3+} ions concentration: (a) $C^{6/3}$, (b) $C^{8/3}$, and (c) $C^{10/3}$

from the Tm^{3+} to Dy^{3+} ions is dominated by the electric multipolar interactions. According to Dexter's energy transfer formula of multipolar interaction and Reisfeld's approximation, the following relationship can be used:[56]

$$\frac{\eta_{S0}}{\eta_S} \propto C^{\alpha/3} \quad (6)$$

Where η_{S0} and η_S represent the luminescence quantum efficiencies of Tm^{3+} ions in the absence and presence of Dy^{3+} ions, respectively. C is the total doping concentration of the Tm^{3+} and Dy^{3+} ions. The value of α = 6, 8, and 10 corresponds to dipole–dipole, dipole–quadrupole, and quadrupole–quadrupole interactions, respectively. The values of η_{S0}/η_S also can be approximately calculated by the ratio of related luminescence intensities as[57]

$$\frac{I_{S0}}{I_S} \propto C^{\alpha/3} \quad (7)$$

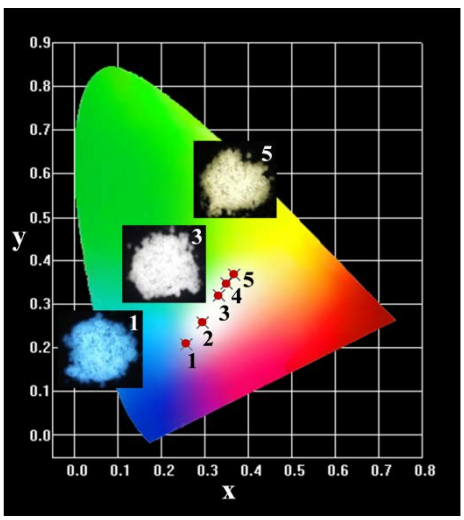

Fig. 14 CIE color coordinate diagram of LGW: 2%Tm^{3+}, x%Dy^{3+} with different Dy^{3+} concentrations: (1) x = 2; (2) x = 4; (3) x = 6; (4) x = 8; and (5) x = 10. The insets are their corresponding digital photographs taken under 365 nm excitation.

Where I_{S0} and I_S refer to the luminescence intensity of Tm^{3+} ions without and with Dy^{3+} ions, respectively. The relationship between I_{S0}/I_S and $C^{\alpha/3}$ based on the above equation is shown in

Fig. 13. It can be clearly seen that when $\alpha = 8$, linear fitting result is the best. Therefore, the energy transfer from Tm^{3+} to Dy^{3+} ions takes place through the dipole–quadrupole interaction mechanism. Fig. 14 shows the CIE chromaticity coordinates and the representative digital luminescence photographs of single-phase emission-tunable phosphors LGW: 2%Tm^{3+}, x%Dy^{3+}. The CIE chromaticity coordinates for the samples were determined on the basis of their corresponding PL spectrum, and were calculated as (0.258, 0.207), (0.294, 0.257), (0.335, 0.321), (0.349, 0.348) and (0.368, 0.368) for LGW: 2%Tm^{3+}, x%Dy^{3+} with x = 2, 4, 6, 8 and 10. For WLED applications, the quantum efficiency (QE) is an important parameter for phosphors. Therefore, the white-light-emitting phosphors, LGW: 2%Tm^{3+}, 4%Tb^{3+}, 3%Eu^{3+} and LGW: 2%Tm^{3+}, 6%Dy^{3+}, are measured. The QE of LGW: 2%Tm^{3+}, 4%Tb^{3+}, 3%Eu^{3+} is 9%, while that of LGW: 2%Tm^{3+}, 6%Dy^{3+} is 28%. It is believed that the quantum efficiency of these white-light-emitting phosphors could be further improved by optimizing the synthetic conditions.

4. Conclusion

In summary, a series of $LiGd(WO_4)_2$: Re^{3+} (Re=Tm, Tb, Dy, Eu) phosphors have been prepared by the conventional solid-state reaction method. Under the excitation of UV light, the LGW: Tm^{3+}, LGW: Tb^{3+}, LGW: Dy^{3+} and LGW: Eu^{3+} phosphors show the characteristic emissions of Tm^{3+} (blue), Tb^{3+} (green), Dy^{3+} (yellow) and Eu^{3+} (red), respectively. More interestingly, two routes are disclosed to realize the white emission *via* the energy transfer process between different rare earth ions in single LGW host. By codoping Tm^{3+}, Tb^{3+}, Eu^{3+} into LGW host, a white light emission was obtained under the excitation of 360 nm which is accessible with UV-LED chips. In addition, the LGW: 2%Tm^{3+}, x%Dy^{3+} phosphors show tunable color from light blue to light yellow, and especially the white light emission is also realized based on energy transfer from Tm^{3+} to Dy^{3+} ions under UV excitation. In details, the energy transfer mechanism from Tm^{3+} to Dy^{3+} ions have been demonstrated to be the dipole–quadrupole interaction. These results indicate that the present materials could potentially serve as single-phase white-light-emitting phosphors for application in UV -excited WLEDs.

Acknowledgements

This work was supported by the National Natural Science Foundation of China (21476045) and the Foundation of key laboratory for micro/nano technology and system of Liaoning province (20140401).

Notes and references

[a] *State Key Laboratory of Fine Chemicals and School of Chemical Engineering, Dalian University of Technology, 2 Linggong Road, Dalian 116012, P. R. China. Fax: +86-0411-84986065 Tel: +86-0411-84986065 E-mail: wtgong@dlut.edu.cn; ninggl@dlut.edu.cn*

[b] *Research Institute of Photonics, Dalian Polytechnic University, Dalian, 116034, P. R. China.*

1 T. R. Kuykendall, A. M. Schwartzberg and S. Aloni, *Adv. Mater*., 2015, DOI:10.1002/adma.201500522.
2 Z. Zhang, D. Liu, D. Li, K. Huang, Y. Zhang, Z. Shi, R. Xie, M.-Y. Han, Y. Wang and W. Yang, *Chem. Mater*., 2015, **27**, 1405.
3 A. Layek, P. C. Stanish, V. Chirmanov and P. V. Radovanovic, *Chem. Mater*., 2015, **27**, 1021.
4 P. Pust, V. Weiler, C. Hecht, A. Tucks, A. S. Wochnik, A. K. Henss, D. Wiechert, C. Scheu, P. J. Schmidt and W. Schnick, *Nat. Mater.*, 2014, **13**, 891.
5 J. Chen, Y. Liu, L. Mei, H. Liu, M. Fang and Z. Huang, *Sci. Rep*., 2015, **5**, 9673.
6 M. M. Shang, C. X. Li and J. Lin, *Chem. Soc. Rev*., 2014, **43**, 1372.
7 S. Nakamura, *Angew. Chem. Int. Ed*., 2015, **54**, 7770.
8 A. Marchuk and W. Schnick, *Angew. Chem. Int. Ed*., 2015, **54**, 2383.
9 X. Li, J. D. Budai, F. Liu, J. Y. Howe, J. Zhang, X.-J. Wang, Z. Gu, C. Sun, R. S. Meltzer and Z. Pan, *Light Sci. Appl*., 2013, **2**, e50.
10 K. Li, M. Shang, Y. Zhang, J. Fan, H. Lian and J. Lin, *J. Mater. Chem. C*, 2015, **3**, 7096.
11 M. H. Fang, H. D. Nguyen, C. C. Lin and R. S. Liu, *J. Mater. Chem. C*, 2015, **3**, 7277.
12 W. Lu, Y. Jia, Q. Zhao, W. Lv and H. You, *Chem.Commun*., 2014, **50**, 2635.
13 J. Ding, Q. Wu, Y. Li, Q. Long, C. Wang and Y. Wang., *Dalton Trans*., 2015, **44**, 9630.
14 G. Li, Y. Zhang, D. Geng, M. Shang, C. Peng, Z. Cheng and J. Lin, *ACS Appl. Mater. Interfaces*., 2012, **4**, 296.
15 H. Liu, Y. Luo, Z. Mao, L. Liao and Z. Xia, *J. Mater. Chem. C*, 2014, **2**, 1619.
16 W. R. Liu, C. H. Huang, C. W. Yeh, J. C. Tsai, Y. C. Chiu, Y. T. Yeh and R. S. Liu, *Inorg Chem.*, 2012, **51**, 9636.
17 W. Tang and F. Zhang, *Eur. J. Inorg. Chem*., 2014, **2014**, 3387.
18 P. Li, Z. Wang, Z. Yang and Q. Guo, *J. Mater. Chem. C*, 2014, **2**, 7823.
19 X. Zhang and M. Gong, *Dalton Trans*., 2014, **43**, 2465.
20 W. Lv, Y. Jia, Q. Zhao, M. Jiao, B. Shao, W. Lü and H. You, *RSC Adv*., 2014, **4**, 7588.
21 Y. Jia, R. Pang, H. Li, W. Sun, J. Fu, L. Jiang, S. Zhang, Q. Su, C. Li and R. S. Liu, *Dalton Trans*., 2015, **44**, 11399.
22 J. Zhou and Z. Xia, *J. Mater. Chem. C*, 2015, **3**, 7552.
23 Z. Ci, Q. Sun, M. Sun, X. Jiang, S. Qin and Y. Wang, *J. Mater. Chem. C*, 2014, **2**, 5850.
24 A. M. Kaczmarek and R. Van Deun, *Chem. Soc. Rev*., 2013, **42**, 8835.
25 X. Liu, W. Hou, X. Yang and J. Liang, *CrystEngComm*., 2014, **16**, 1268.
26 Y. Liu, G. Liu, J. Wang, X. Dong and W. Yu, *Inorg. Chem*., 2014, **53**, 11457.
27 Z. Wang, J. Zhong, H. Jiang, J. Wang and H. Liang, *Cryst. Growth Des*., 2014, **14**, 3767.
28 B. Rekik, M. Derbal, O. Benamara and K. Lebbou, *J. Cryst. Growth*., 2014, **405**, 11.
29 X. Huang, Z. Lin, L. Zhang, J. Chen and G. Wang, *Cryst. Growth Des*., 2006, **6**, 2271.
30 J. M. Postema, W. T. Fu and D. J. W. Ijdo, *J.Solid.State.Chem*., 2011, **184**, 2004.
31 L. Li, Y. Liu, R. Li, Z. Leng and S. Gan., *RSC Adv*., 2015, **5**, 7049.
32 A. J. Peter and I. B. Shameem Banu, *J. Mater. Sci.: Mater. Electron*., 2014, **25**, 2771.
33 G. Li, C. Li, C. Zhang, Z. Cheng, Z. Quan, C. Peng and J. Lin, *J. Mater. Chem*, 2009, **19**, 8936.
34 L. Wu, Y. Zhang, M. Y. Gui, P. Z. Lu, L. X. Zhao, S. Tian, Y. F. Kong and J. J. Xu, *J. Mater. Chem*., 2012, **22**, 6463.
35 H. Qian, J. Zhang and L. Yin, *RSC Adv*., 2013, **3**, 9029.
36 L. Hou, S. Cui, Z. Fu, Z. Wu, X. Fu and J. H. Jeong, *Dalton Trans*., 2014, **43**, 5382.
37 L. Jing, X. Liu, Y. Li and Y. Wang, *J. Lumin*., 2015, **162**, 185.
38 Y. Zhang, W. Gong, J. Yu, H. Pang, Q. Song and G. Ning, *RSC Adv*., 2015, **5**, 62527.
39 T. Ishigaki, A. Torisaka, K. Nomizu, P. Madhusudan, K. Uematsu, K. Toda and M. Sato, *Dalton Trans*., 2013, **42**, 4781.
40 Y. Luo, Z. Xia, B. Lei and Y. Liu, *RSC Adv.*, 2013, **3**, 22206.
41 Y. Su, L. Li and G. Li, *J. Mater. Chem*, 2009, **19**, 2316.
42 X. Li, Y. Zhang, D. Geng, J. Lian, G. Zhang, Z. Hou and J. Lin, *J. Mater. Chem. C*, 2014, **2**, 9924.
43 Nakazawa, E.; Shionoya, S. *J. Chem. Phys*., 1967, **47**, 3211.
44 C. Lorbeer and A. V. Mudring, *J. Phys. Chem. C*, 2013, **117**, 12229.
45 J. Zhou and Z. Xia, *J. Mater. Chem. C*, 2014, **2**, 6978.

46 Z. Hou, Z. Cheng, G. Li, W. Wang, C. Peng, C. Li, P. Ma, D. Yang, X. Kang and J. Lin, *Nanoscale.*, 2011, **3**, 1568.
47 G. Li, Z. Hou, C. Peng, W. Wang, Z. Cheng, C. Li, H. Lian and J. Lin, *Adv. Funct. Mater*., 2010, **20**, 3446.
48 K. Li, Y. Zhang, X. Li, M. Shang, H. Lian and J. Lin, *Phys. Chem. Chem. Phys.*, 2015, **17**, 4283.
49 S. P. Lee, C. H. Huang and T. M. Chen, *J. Mater. Chem. C*, 2014, **2**, 8925.
50 C. H. Huang and T. M. Chen, *J. Phys. Chem. C*, 2011, **115**, 2349.
51 W. Wu and Z. Xia, *RSC Adv*., 2013, **3**, 6051.
52 S. Das, C. Y. Yang, H. C. Lin and C. H. Lu, *RSC Adv*., 2014, **4**, 64956.
53 G. Blasse, *Philips Res. Rep*., 1969, **24**, 131.
54 R. Reisfeld, L. Boehm, *J. Solid State Chem*., 1972, **4**, 417.
55 W. J. Yang, L. Y. Luo, T. M. Chen and N. S. Wang, *Chem. Mater*., 2005, **17**, 3883.
56 D. L. Dexter and J. A. Schulman, *J. Chem. Phys*., 1954, **22**, 1063.
57 J. Sun, Z. Lian, G. Shen and D. Shen, *RSC Adv*., 2013, **3**, 18395.